On the Color Dipole Picture at low-x DIS

Dieter Schildknecht

Universität Bielefeld & Max Planck Institut für Physik, München

Prospects for a very high energy eP and eA Collider
MPI Physik München, June 1 – 2, 2017

1. Deep Inelastic ep Scattering

Experimental Results

Deep inelastic scattering (DIS), HERA 1992 to 2007:

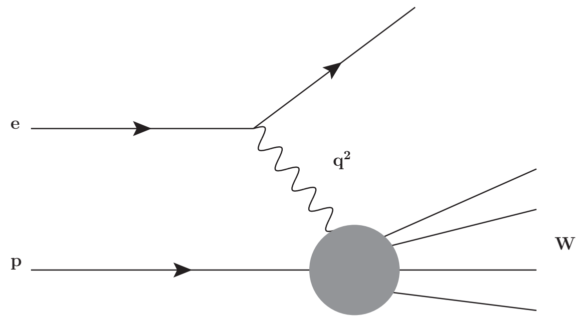

DIS at low values of

$$x \equiv x_{bj} \simeq \frac{Q^2}{W^2}, \text{ where}$$
$$5 \cdot 10^{-4} \le x \le 10^{-1}$$
$$0 \le Q^2 \le 100 GeV^2$$

$$Q^2 \equiv -q^2 > 0,$$
$$x_{bj} = \frac{Q^2}{W^2 + Q^2 + M_p^2} \cong \frac{Q^2}{W^2}.$$

$$\sigma_{\gamma^* p}(W^2, Q^2) = \sigma_{\gamma_L^* p}(W^2, Q^2) + \sigma_{\gamma_T^* p}(W^2, Q^2)$$
$$\equiv \sigma_{\gamma_T^* p}(W^2, Q^2)(1 + R(W^2, Q^2)),$$

$$F_2(x, Q^2) \cong \frac{Q^2}{4\pi^2 \alpha} \sigma_{\gamma^* p}(W \cong \frac{Q^2}{x}, Q^2);$$
$$F_L = \frac{R}{1+R} F_2.$$

Low-x Scaling

$$\text{Empirically}: \qquad \eta(W^2, Q^2) \equiv \frac{Q^2 + m_0^2}{\Lambda^2_{sat}(W^2)},$$

$$\Lambda^2_{sat}(W^2) \sim (W^2)^{C_2}$$

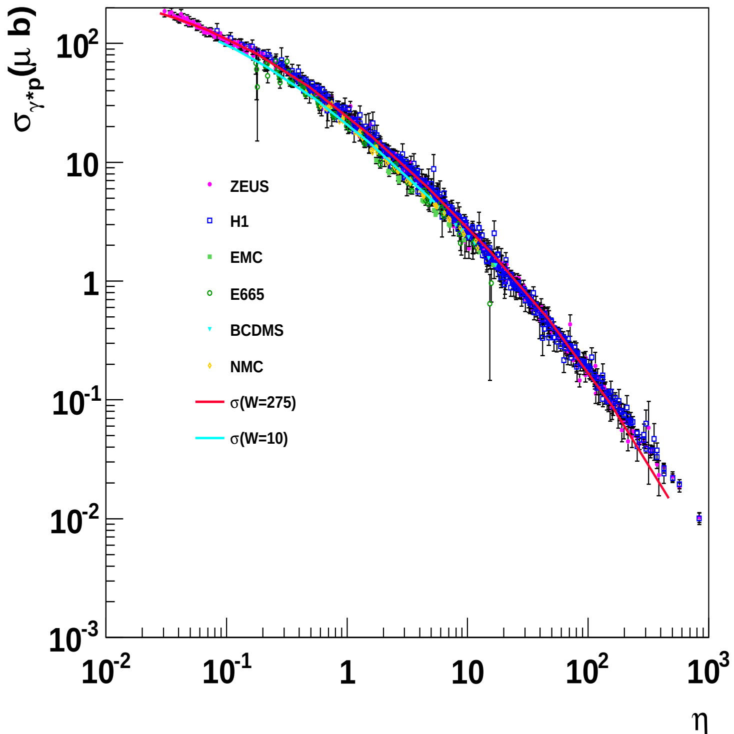

Schildknecht, Surrow, Tentyukov (2000)

$$\sigma_{\gamma^* p}(W^2, Q^2) \;=\; \sigma_{\gamma^* p}(\eta(W^2, Q^2))$$

$$\sim\; \sigma^{(\infty)} \begin{cases} ln\frac{1}{\eta(W^2,Q^2)} & , \quad \text{for } \eta(W^2, Q^2) \ll 1 \\ \frac{1}{\eta(W^2,Q^2)} & , \quad \text{for } \eta(W^2, Q^2) \gg 1 \end{cases}$$

The W-dependence

$$F_2(x,Q^2) \cong \frac{Q^2}{4\pi^2\alpha}\left(\sigma_{\gamma^*_L p}(W^2,Q^2)+\sigma_{\gamma^*_T p}(W^2,Q^2)\right)$$

$$= F_2(W^2) \;\; \text{for} \;\; x < 0.1. \qquad (10GeV^2 \leq Q^2 \leq 100GeV^2)$$

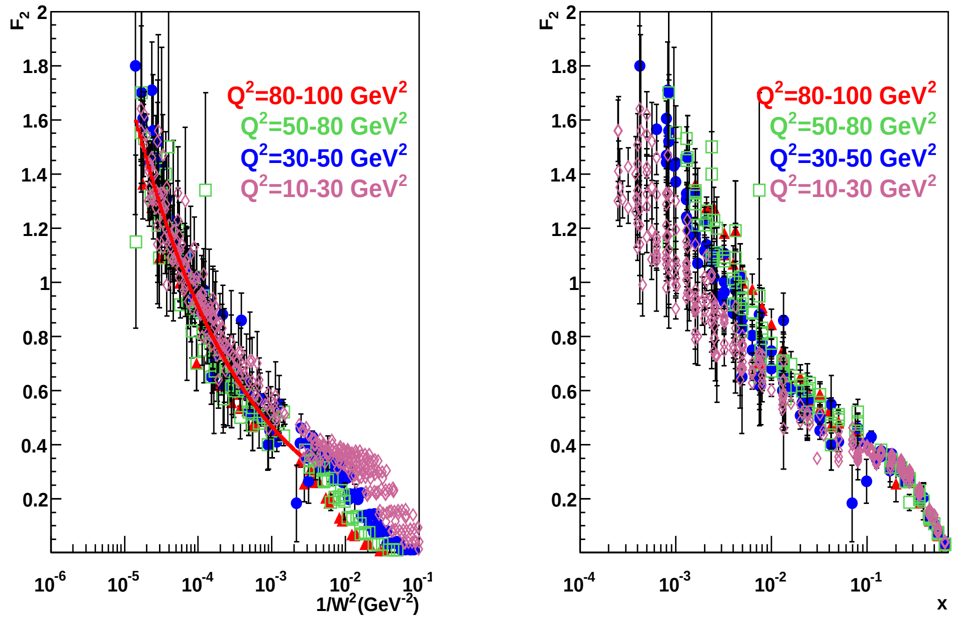

$$F_2(W^2) = f_2\left(\frac{W^2}{1GeV^2}\right)^{c_2=0.29},$$

$$f_2 = 0.063.$$

Kuroda, Schildknecht (2010)

(Prabhdeep Kaur)

The limit of $\eta(W^2,Q^2) \to 0$, or $W^2 \to \infty$ at Q^2 fixed ("saturation")

$$\lim_{\substack{W^2\to\infty \\ Q^2 \ \text{fixed}}} \frac{\sigma_{\gamma^* p}(\eta(W^2,Q^2))}{\sigma_{\gamma^* p}(\eta(W^2,Q^2=0))} = \lim_{\substack{W^2\to\infty \\ Q^2 \ \text{fixed}}} \frac{\ln\left(\frac{\Lambda^2_{sat}(W^2)}{m_0^2}\frac{m_0^2}{(Q^2+m_0^2)}\right)}{\ln\frac{\Lambda^2_{sat}(W^2)}{m_0^2}} = 1 + \lim_{\substack{W^2\to\infty \\ Q^2 \ \text{fixed}}} \frac{\ln\frac{m_0^2}{Q^2+m_0^2}}{\ln\frac{\Lambda^2_{sat}(W^2)}{m_0^2}} = 1.$$

$$\sigma_{\gamma^* p}\left(\eta(W^2,Q^2=0)\right) = \sigma_{\gamma p}(W^2)$$

D. Schildknecht, DIS 2001 (Bologna)

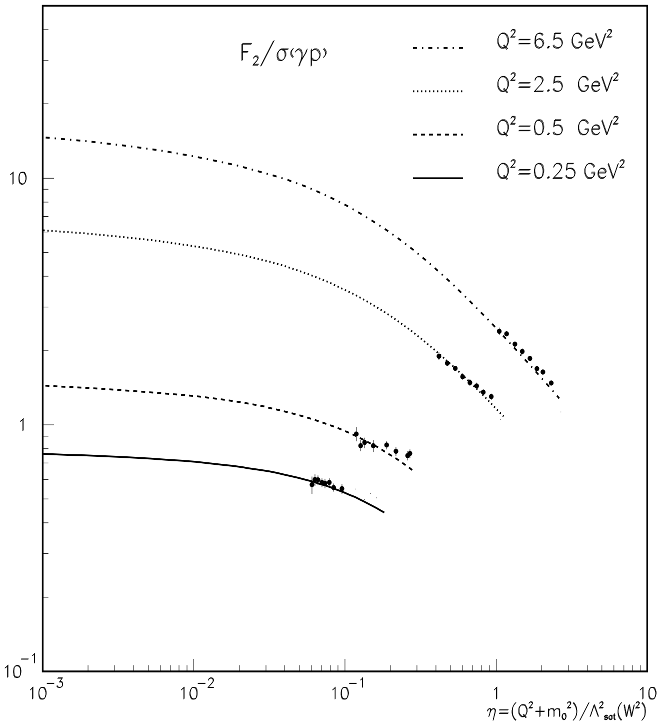

$\mathrm{Q^2[GeV^2]}$	$\mathrm{W^2[GeV^2]}$	$\frac{\sigma_{\gamma^* p}(\eta(\mathrm{W^2},\mathrm{Q^2}))}{\sigma_{\gamma p}(\mathrm{W^2})}$
1.5	2.5×10^7	0.5
	1.26×10^{11}	0.63

$$\lim_{\substack{W^2\to\infty \\ Q^2 \text{fixed}}} \frac{F_2(x\cong Q^2/W^2,Q^2)}{\sigma_{\gamma p}(W^2)} = \frac{Q^2}{4\pi^2\alpha}.$$

for $\eta = 10^{-2}$:

$\mathrm{Q^2[GeV^2]}$	$\Lambda^2_{\mathrm{sat}}(\mathrm{W^2})[\mathrm{GeV^2}]$	W[GeV]
0.5	65	1.7×10^4
2.5	265	2.2×10^5

VHEeP: W $\sim 10^4$GeV

The experimentally observed behavior

follows from the Color Dipole Picture (CDP)

of deep-inelastic scattering for $x \lesssim 0.1$.

The Color Dipole Picture (CDP).

The longitudinal and the transverse photoabsorption cross section

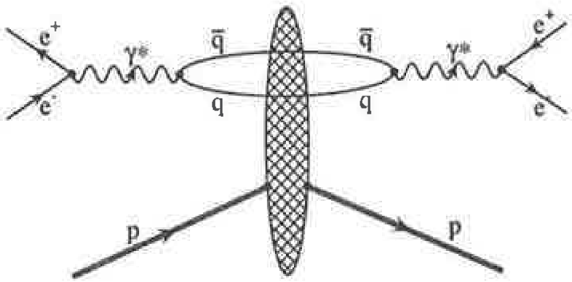

(a)

channel 1:

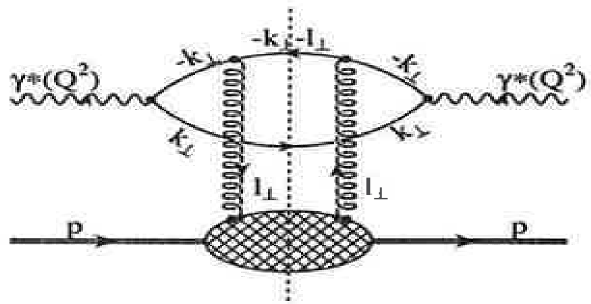

(a)

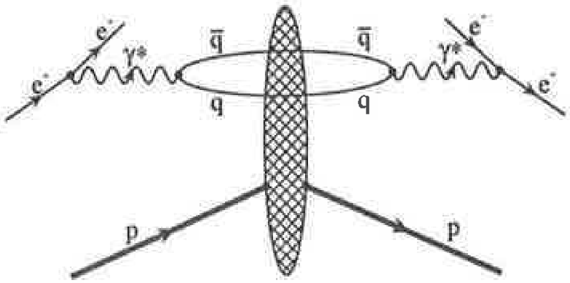

(b)

channel 2:

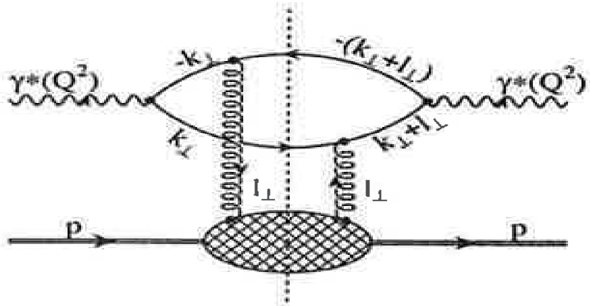

(b)

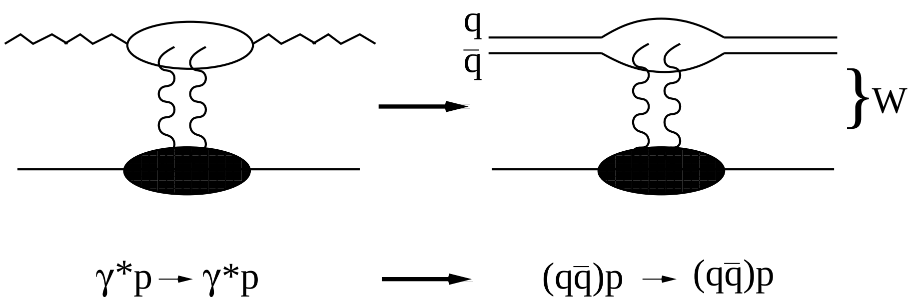

$$\tau = \frac{1}{\Delta E} \cong \frac{1}{x + \frac{M^2_{q\bar{q}}}{W^2}} \frac{1}{M_p} \gg \frac{1}{M_p}$$

(A) $\sigma_{\gamma^*_{L,T}}(W^2, Q^2) = \int dz \int d^2\vec{r}_\perp |\psi_{L,T}(\vec{r}_\perp, z(1-z), Q^2)|^2 \;\; \sigma_{(q\bar{q})p}(\vec{r}_\perp, z(1-z), W^2)$

Remarks:

i) $|\psi_{L,T}(\vec{r}_\perp, z(1-z), Q^2)|$: Probability for $\gamma^*_{L,T} \to q\bar{q}$ fluctuation (QED)

Note: $\vec{r}_\perp^{\,2} \sim \frac{1}{Q^2}$

ii) $\sigma_{(q\bar{q})p}(\vec{r}_\perp, z(1-z), W^2)$: $(q\bar{q})p$ cross section dependent on W^2 (not on $x \equiv \frac{Q^2}{W^2}$)

$\tau \equiv \frac{1}{\Delta E} = \frac{1}{x + \frac{M^2_{q\bar{q}}}{W^2}} \frac{1}{M_p} \gg \frac{1}{M_p}$

$x \simeq \frac{Q^2}{W^2}$

Generalized Vector Dominance

Sakurai, Schildknecht 1972

W^2-Dependence: Ewerz and Nachtmann 2006

(B) Gauge-invariant two-gluon coupling (QCD):

$$\sigma_{(q\bar{q})p}(\vec{r}_\perp, z(1-z), W^2) = \int d^2\vec{l}_\perp \tilde{\sigma}(\vec{l}_\perp^{\,2}, z(1-z), W^2)\left(1 - e^{-i\,\vec{l}_\perp\cdot\vec{r}_\perp}\right)$$

Low (1975)

Nussinov (1975)

Nikolaev, Zakharov (1991)

Cvetic, Schildknecht, Shoshi(2000)

Assume $\vec{l}_\perp^{2} \le \vec{l}_{\perp \mathrm{Max}}^{2}(W^2)$.

For fixed $|\vec{r}_\perp|$:

a) $\vec{l}_{\perp \mathrm{Max}}^{2}(W^2)\vec{r}_\perp^{\,2} \ll 1$

$\sigma_{(q\bar{q})p} \sim \vec{r}_\perp^{\,2}$, "color transparency", $\xrightarrow[(A)]{} \sigma_{\gamma^* p} \sim \frac{1}{\eta(W^2,Q^2)} \sim \frac{\Lambda^2_{\mathrm{sat}}(W^2)}{Q^2}$.

b) $\vec{l}_{\perp \mathrm{Max}}^{2}(W^2)\vec{r}_\perp^{\,2} \gg 1$

$\sigma_{(q\bar{q})p} \sim \sigma^{(\infty)}(W^2)$, "saturation" $\xrightarrow[(A)]{} \sigma_{\gamma^* p} \sim \ln \frac{1}{\eta(W^2,Q^2)}$;

Color gauge invariant $q\bar{q}$ (dipole) interaction with gluon field in the nucleon implies low-x scaling.

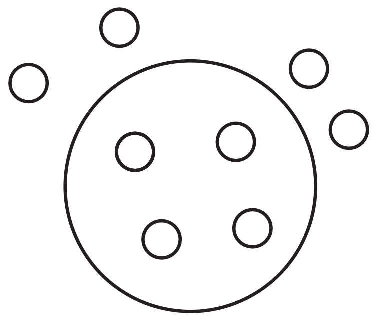

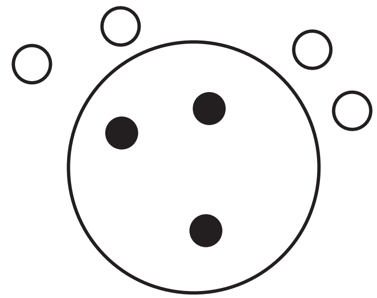

Color Transparency

$$\eta(W^2, Q^2) \simeq \frac{Q^2}{\Lambda^2_{\rm sat}(W^2)} \gg 1$$

Saturation

hadron-like cross section

$$\eta(W^2, Q^2) \lesssim 1$$

The (Q^2, W^2) plane of low-x DIS in CDP.

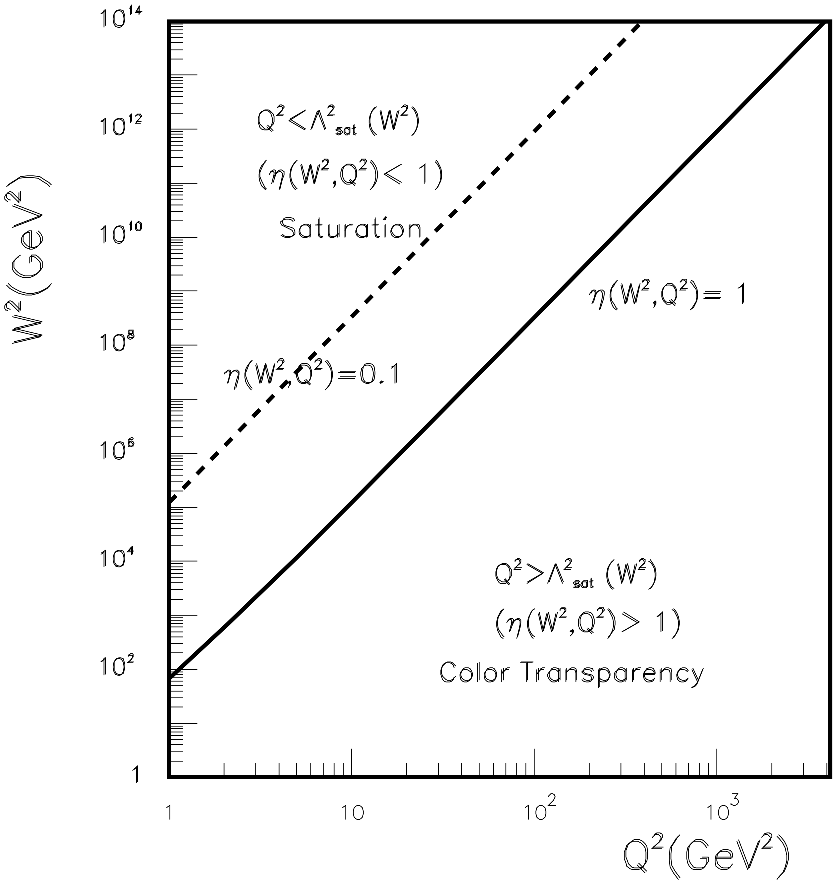

The longitudinal-to-transverse ratio

$(q\bar{q})^{J=1}_{L,T}$ states : $\gamma^*_{L,T} \longrightarrow (q\bar{q})^{J=1}_{L,T}$

$$\sigma_{\gamma^*_{L,T}p}(W^2, Q^2) = \alpha \sum_q Q_q^2 \frac{1}{Q^2}\frac{1}{6} \begin{cases} \int d\vec{l}_\perp^{\prime 2} \vec{l}_\perp^{\prime 2} \bar{\sigma}_{(q\bar{q})^{J=1}_{L}p}(\vec{l}_\perp^{\prime 2}, W^2), \\ 2 \int d\vec{l}_\perp^{\prime 2} \vec{l}_\perp^{\prime 2} \bar{\sigma}_{(q\bar{q})^{J=1}_{T}p}(\vec{l}_\perp^{\prime 2}, W^2). \end{cases} \quad (\text{for } \eta \gg 1)$$

$$\vec{l}^2 = z(1-z)\vec{l}_\perp^2$$

$$\rho_W = \frac{\int d\vec{l}_\perp^{\prime 2} \vec{l}_\perp^{\prime 2} \bar{\sigma}_{(q\bar{q})^{J=1}_{T}p}(\vec{l}_\perp^{\prime 2}, W^2)}{\int d\vec{l}_\perp^{\prime 2} \vec{l}_\perp^{\prime 2} \bar{\sigma}_{(q\bar{q})^{J=1}_{L}p}(\vec{l}_\perp^{\prime 2}, W^2)} . \equiv \rho$$

$$R = \frac{1}{2\rho}.$$

Magnitude of ρ

Average transverse momentum of $q(\bar{q})$:

$$\langle \vec{l}_\perp^{\,2} \rangle_{L,T}^{\vec{l}_\perp^{\prime 2}=const} = \vec{l}_\perp^{\prime 2} \begin{cases} 6 \int dz z^2 (1-z)^2 = \frac{4}{20} \vec{l}_\perp^{\prime 2}, & (L) \\ \frac{3}{2} \int dz \; z(1-z)(1 - 2z(1-z)) = \frac{3}{20} \vec{l}_\perp^{\prime 2}, & (T) \end{cases} .$$

Assume that ρ is determined by average transverse size of $L(T)$. Uncertainty principle:

$$\rho = \frac{\langle \vec{r}_\perp^{\,2} \rangle_T}{\langle \vec{r}_\perp^{\,2} \rangle_L} = \frac{\langle \vec{l}_\perp^{\,2} \rangle_L}{\langle \vec{l}_\perp^{\,2} \rangle_T} = \frac{4}{3}.$$

Kuroda, Schildknecht (2008)

$$R = \frac{1}{2\rho} = \begin{cases} 0.5 & \text{for } \rho = 1, \\ \frac{1 \cdot 3}{2 \cdot 4} = \frac{3}{8} = 0.375 & \text{uncertainty principle} \\ \frac{1}{4}, & \text{for } \rho = 2. \end{cases}$$

$$F_L = \frac{R}{1+R} = \begin{cases} 0.33 \\ 0.27 \\ 0.20 \end{cases}$$

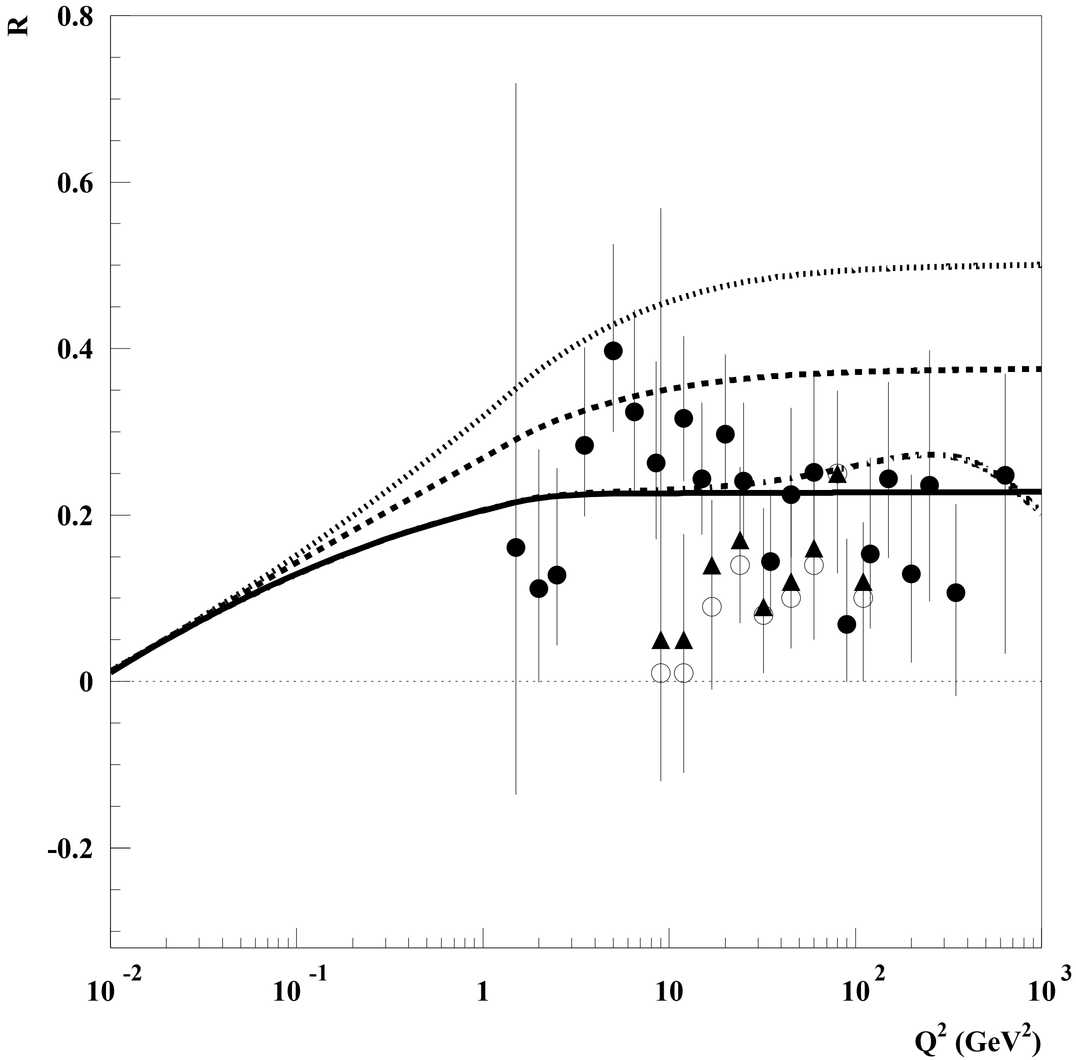

Experiment: $R(Q^2)|_{W\simeq 200\ \mathrm{GeV}}$

H1 (2013)

ZEUS (2014)

Theory (CDP)

$\longleftarrow$ $\rho = 1$

$\longleftarrow$ $\rho = \frac{4}{3}$ (uncertainty principle)

$\longleftarrow$ $\rho = 2$

So far: Model-independently:

$$\sigma_{\gamma^* p} \sim \begin{cases} ln \frac{1}{\eta(W^2,Q^2)} & , \quad \eta(W^2,Q^2) \ll 1 \\ \frac{1}{\eta(W^2,Q^2)} & , \quad \eta(W^2,Q^2) \gg 1 \end{cases}$$

$$R = \begin{cases} 0 & \text{for } Q^2 = 0, \left(\eta = \frac{m_0^2}{\Lambda^2_{\rm sat}(W^2)}\right), \\ \frac{1}{2\rho} & \qquad \text{for } \eta(W^2,Q^2) \gg 1. \end{cases}$$

Interpolation between $\eta(W^2,Q^2) < 1$ and $\eta(W^2,Q^2) > 1$ by explicit ansatz for the dipole cross section.

Simple ansatz for $\sigma_{(q\bar{q})p}$ cross section

$$\tilde{\sigma}\left(\vec{l}_\perp^{\,2}, z(1-z), W^2\right) = \frac{\sigma^{(\infty)}(W^2)}{\pi}\delta\left(\vec{l}_\perp^{\,2} - z(1-z)\Lambda^2_{sat}(W^2)\right)$$

Cvetic, Schildknecht, Surrow, Tentyukov (2001)

Kuroda, Schildknecht (2011)

and arXiv: 1606.07862.

$$\sigma_{\gamma^* p}(W^2, Q^2) = \frac{\sigma_{\gamma p}(W^2)}{\lim\limits_{\eta\to\mu(W^2)} I_T^{(1)}\left(\frac{\eta}{\rho}, \frac{\mu}{\rho}\right)} \left(I_T^{(1)}\left(\frac{\eta}{\rho}, \frac{\mu}{\rho}\right) G_T(u) + I_L^{(1)}(\eta, \mu) G_L(u)\right)$$

$$G_{L,T}(u) = \frac{1}{2(1+u)^3}\begin{cases} 2u^3 + 6u^2, & (L), \\ 2u^3 + 3u^2 + 3u, & (T). \end{cases}$$

$$u = \frac{\xi}{\eta(W^2, Q^2)}; \qquad \mu(W^2) = \frac{m_0^2}{\Lambda^2_{\rm sat}(W^2)}.$$

$$m^2_{q\bar{q}} \le m_1^2(W^2) = \xi\Lambda^2_{\rm sat}(W^2).$$

$$
\begin{aligned}
I_L^{(1)}(\eta,\mu) &= \frac{\eta-\mu}{\eta} \\
&\times\left(1-\frac{\eta}{\sqrt{1+4(\eta-\mu)}}\ln\frac{\eta(1+\sqrt{1+4(\eta-\mu)})}{4\mu-1-3\eta+\sqrt{(1+4(\eta-\mu))((1+\eta)^2-4\mu)}}\right),
\end{aligned}
$$

$$
I_T^{(1)}(\eta,\mu) = \frac{1}{2}\ln\frac{\eta-1+\sqrt{(1+\eta)^2-4\mu}}{2\eta} - \frac{\eta-\mu}{\eta} + \frac{1+2(\eta-\mu)}{2\sqrt{1+4(\eta-\mu)}}
$$

$$
\times\ln\frac{\eta(1+\sqrt{1+4(\eta-\mu)})}{4\mu-1-3\eta+\sqrt{(1+4(\eta-\mu))((1+\eta)^2-4\mu)}}.
$$

Comparison with experiment: Kuroda, Schildknecht (2011)

- $\sigma_{\gamma p}(W^2)$ from Particle Data Group parameterization

- $\Lambda^2_{sat}(W^2) = C_1 \left(\frac{W^2}{W_0^2} + 1\right)^{C_2} \cong$ const $\left(\frac{W^2}{1GeV^2}\right)^{C_2} = 0.31(W^2)^{0.27}$

$C_1 = 1.95GeV^2 \qquad m_0^2 = 0.15GeV^2$

$W_0^2 = 1081GeV^2 \qquad m_1^2(W^2) = \xi\Lambda^2_{sat}(W^2) = 130\Lambda^2_{sat}(W^2)$

$C_2 = 0.27(0.29)$

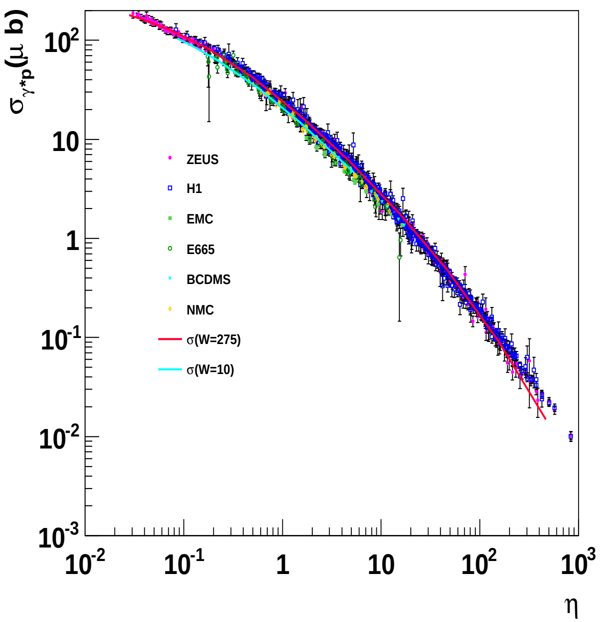

3. Very High Energy eP Scattering

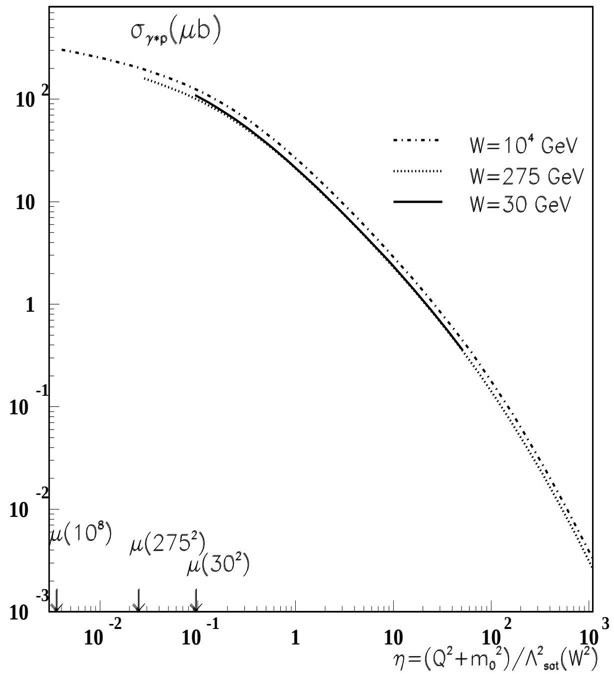

$$\sigma_{\gamma^* p}(W^2, Q^2) = \frac{\alpha R_{e^+e^-}}{3\pi}\sigma^{(\infty)}(W^2) I_0\left(\eta(W^2, Q^2)\right)$$

$$\cong \frac{\alpha R_{e^+e^-}}{3\pi}\sigma^{(\infty)}(W^2) \ln\left(\frac{1}{\eta(W^2, Q^2)}\right),$$

for $\eta(W^2, Q^2) \ll 1$.

Smooth transition to $Q^2 = 0$:

$$\sigma_{\gamma^* p}(W^2, Q^2) = \frac{\sigma_{\gamma p}(W^2)}{\ln \frac{\Lambda^2_{sat}(W^2)}{m_0^2}} I_0(\eta(W^2, Q^2)) \xrightarrow[Q^2 \to 0]{} \sigma_{\gamma p}(W^2).$$

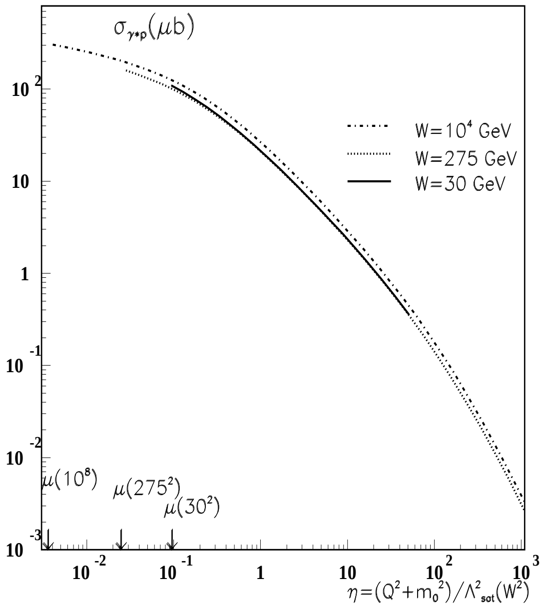

Photoproduction:

$\boldsymbol{\sigma_{\gamma p}(W^2)}$ **from measurements of** $\boldsymbol{\sigma^{(\infty)}(W^2)}$

$$\sigma_{\gamma p}(W^2) = \frac{\alpha R_{e^+e^-}}{3\pi} \ln\left(\frac{\Lambda^2_{sat}(W^2)}{m_0^2}\right) \sigma^{(\infty)}(W^2)$$

$$\text{e.g. } \sigma^{(\infty)}(W^2) \simeq \begin{cases} \ln(W^2) & \xrightarrow[\text{“hadronlike”}]{} \sigma_{\gamma p}(W^2) \sim (\ln(W^2))^2 \\ \text{const} & \xrightarrow{\qquad} \sigma_{\gamma p}(W^2) \sim (\ln(W^2)) \end{cases}$$

“hadronlike”: $(\ln W^2)^2$, Heisenberg 1953

Froissart 1961

The limit of $\eta(W^2, Q^2) \to 0$, or $W^2 \to \infty$ at Q^2 fixed ("saturation")

$$\lim_{\substack{W^2\to\infty \\ Q^2 \ \text{fixed}}} \frac{\sigma_{\gamma^* p}(\eta(W^2,Q^2))}{\sigma_{\gamma^* p}(\eta(W^2,Q^2=0))} = \lim_{\substack{W^2\to\infty \\ Q^2 \ \text{fixed}}} \frac{\ln\left(\frac{\Lambda^2_{sat}(W^2)}{m_0^2}\frac{m_0^2}{(Q^2+m_0^2)}\right)}{\ln \frac{\Lambda^2_{sat}(W^2)}{m_0^2}} = 1 + \lim_{\substack{W^2\to\infty \\ Q^2 \ \text{fixed}}} \frac{\ln \frac{m_0^2}{Q^2+m_0^2}}{\ln \frac{\Lambda^2_{sat}(W^2)}{m_0^2}} = 1.$$

$$\sigma_{\gamma^* p}\left(\eta(W^2, Q^2=0)\right) = \sigma_{\gamma p}(W^2)$$

D. Schildknecht, DIS 2001 (Bologna)

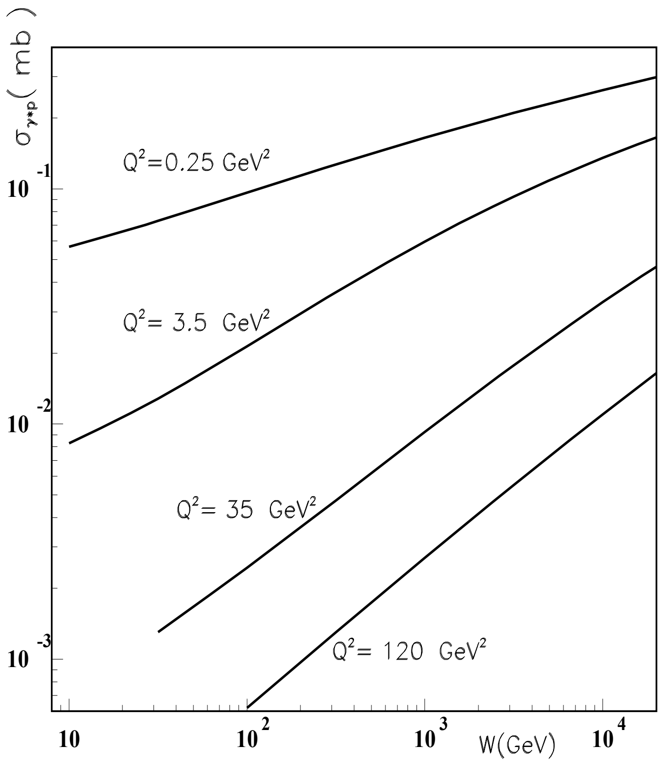

4. The Mass Range of "active" $\gamma^* \to q\bar{q}$ Fluctuations

$$\tau \simeq \frac{1}{x_{bj} + \frac{M^2_{q\bar{q}}}{W^2}} \frac{1}{M_p} \gg \frac{1}{M_p}$$

Thus: $M^2_{q\bar{q}} \le m^2_1(W^2) = \xi \Lambda^2_{sat}(W^2)$

Empirically: $\xi_{Exp} \cong 130$

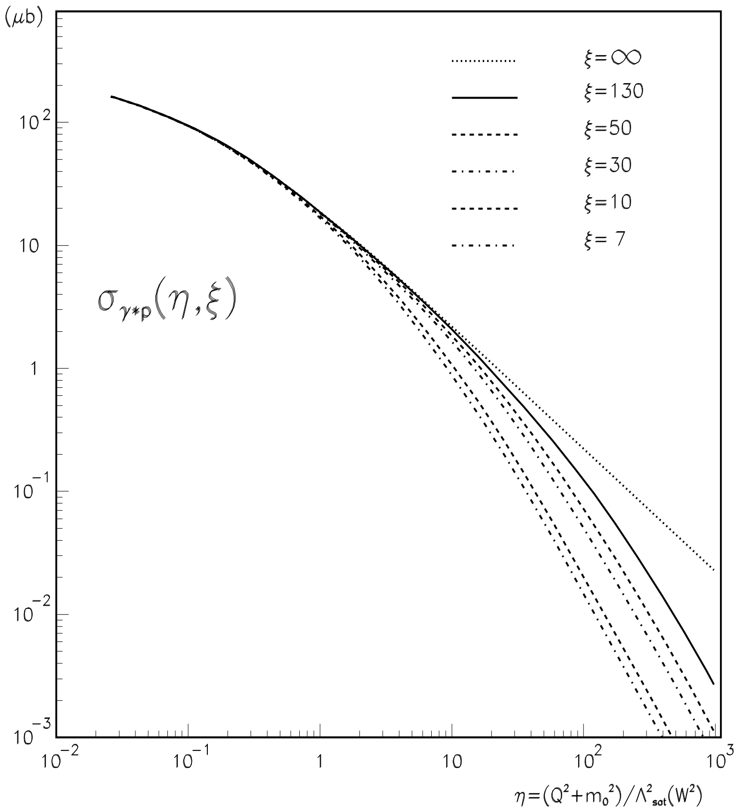

(i) $\eta(W^2, Q^2) \gtrsim 10$: $\xi_{exp} \cong 130$.

Very-high-mass states not contributing.

High-mass states necessary

(ii) $\eta(W^2, Q^2) \lesssim 10$:

For $\eta(W^2, Q^2) \rightarrow \eta_{Min}(W^2, Q^2 = 0)$

$= \frac{m_0^2}{\Lambda^2_{sat}(W^2)}$

decreasing $q\bar{q}$ masses "active".

Consider fixed $\eta(W^2, Q^2) \lesssim 10$.

Dependence on $\frac{\eta(W^2,Q^2)}{\xi} < 1$:

$$\sigma_{\gamma^* p}\left(\eta(W^2, Q^2), \frac{\eta(W^2,Q^2)}{\xi}\right) \cong \sigma_{\gamma^* p}\left(\eta(W^2, Q^2, \frac{\eta(W^2,Q^2)}{\xi} \to 0\right)\left(1 - \frac{3}{2} \quad \frac{\eta(W^2,Q^2)}{\xi}\right).$$

"Active" $q\bar{q}$ fluctuations: **Fraction $(1 - \epsilon)$ of experimentally observed cross sections (e.g. $\epsilon = 0.1$):**

$$\xi = \frac{3}{2}\frac{\eta(W^2, Q^2)}{\epsilon};$$

$$\begin{aligned} m_0^2 \leq M_{q\bar{q}}^2 \ \leq \ & \frac{3}{2\epsilon}\eta(W^2, Q^2)\Lambda_{sat}^2(W^2) \\ = \ & \frac{3}{2\epsilon}(Q^2 + m_0^2) \\ = \ & 15(Q^2 + m_0^2) \quad \text{for e.g.} \quad \epsilon = 0.1. \end{aligned}$$

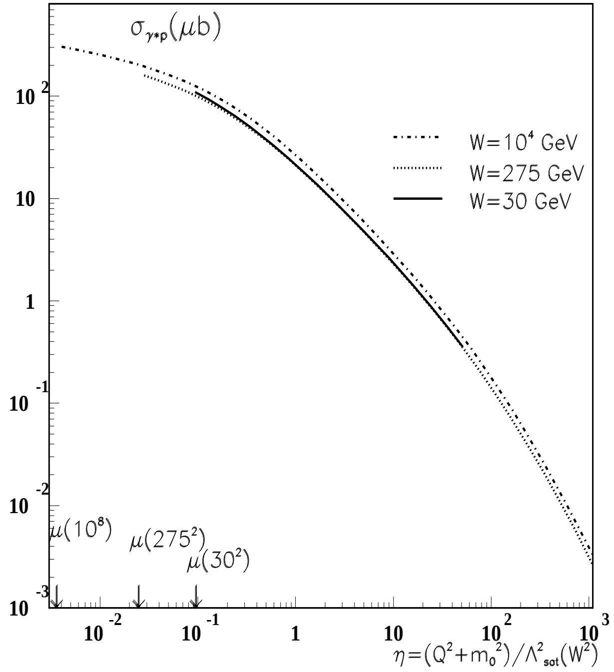

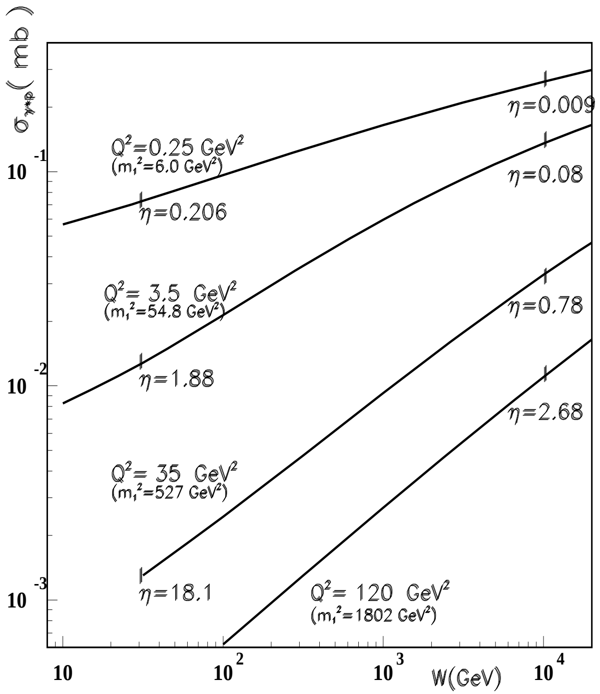

Transition from Color Transparency, $\eta(W^2, Q^2) \gtrsim 1$

to Saturation, $\eta(W^2, Q^2) \lesssim 1$

$$m_0^2 \le M_{q\bar{q}}^2 \le m_1^2 = \frac{3}{2\epsilon}\eta(W^2, Q^2)\Lambda^2_{sat}(W^2) = \frac{3}{2\epsilon}(Q^2 + m_0^2)$$

W [Gev] $\Lambda^2_{sat}(W^2)[\mathrm{GeV}^2]$	30 1.95	300 6.75	10^4 44.8
$Q^2 = 10\ \mathrm{GeV}^2$ $m_1^2 = 152\ \mathrm{GeV}^2$ $m_1 = 12.3\ \mathrm{GeV}$	5.2	1.5	2.3×10^{-1}
$Q^2 = 2\ \mathrm{GeV}^2$ $m_1^2 = 32.3\ \mathrm{GeV}^2$ $m_1 = 5.68\ \mathrm{GeV}$	1.1	3.2×10^{-1}	4.8×10^{-2}
$Q^2 = 0$ $m_1^2 = 2.25\ \mathrm{GeV}^2$ $m_1 = 1.5\ \mathrm{GeV}$	7.7×10^{-2}	2.2×10^{-2}	3.3×10^{-3}

Table: Values of $\eta(W^2, Q^2)$.

Mass Range: $M^2_{q\bar{q}} \leq m_1^2 = \frac{3}{2\epsilon}(Q^2 + m_0^2)$ with $\epsilon = 0.1$.

W [Gev] $\Lambda^2_{sat}(W^2)$[GeV^2] $\eta_{Min}(W^2)$	30 1.95 7.6×10^{-2}	300 6.75 2.2×10^{-2}	10^4 44.8 3.3×10^{-3}
$\eta = 1$	$Q^2 = 1.8$ GeV^2 $m_1^2 = 29$ GeV^2 $m_1 = 5.4$ GeV	$Q^2 = 6.9$ GeV^2 $m_1^2 = 101$ GeV^2 $m_1 = 10$ GeV	$Q^2 = 44.7$ GeV^2 $m_1^2 = 672$ GeV^2 $m_1 = 25$ GeV
$\eta = 0.1$	$Q^2 = 4.5 \times 10^{-2}$ $m_1^2 = 2.9$ GeV^2 $m_1 = 1.7$ GeV	$Q^2 = 0.53$ GeV^2 $m_1^2 = 10.1$ GeV^2 $m_1 = 3.2$ GeV	$Q^2 = 4.3$ GeV^2 $m_1^2 = 67$ GeV^2 $m_1 = 8.2$ GeV
$\eta = \eta_{Min}$	$Q^2 = 0$ $m_1^2 = 2.25$ GeV^2 $m_1 = 1.5$ GeV		

Table: Mass Range $M^2_{q\bar{q}} \leq m_1^2$ for given $\eta(W^2, Q^2)$ as a function of W.

A Remark on : $F_2(W^2)$ in terms of gluon distribution:

$$F_2(W^2 = \frac{Q^2}{x}) = \frac{(2\rho+1)\sum Q_q^2}{3\pi}\xi_L^{C_2}\alpha_s(Q^2)G(x,Q^2) \qquad \eta(W^2,Q^2) \gg 1.$$

$$= \frac{(2\rho+1)\sum Q_q^2}{3\pi}\frac{1}{8\pi^2}\sigma_L^{(\infty)}\Lambda_{sat}^2(W^2). \qquad \text{color transparency}$$

(upon using $F_2 = f_2\left(\frac{W^2}{1GeV^2}\right)^{0.29} = \frac{(2\rho+1)\sum Q_q^2}{3\pi}\frac{1}{8\pi^2}\sigma_L^{(\infty)}\Lambda_{sat}^2(W^2)$.)

Saturation behavior:

$$F_2(W^2,Q^2) \sim Q^2\sigma_L^{(\infty)}\ln\frac{\Lambda_{\rm sat}^2(W^2)}{Q^2+m_0^2}$$

$$\sim Q^2\sigma_L^{(\infty)}\ln\left(\frac{\alpha_s(Q^2)G(x,Q^2)}{\sigma_L^{(\infty)}(Q^2+m_0^2)}\right), \qquad \eta(W^2,Q^2) \ll 1.$$

saturation

Logarithmic dependence on gluon distribution in saturation limit.

5. Photo- and Electroproduction of J/ψ and Y

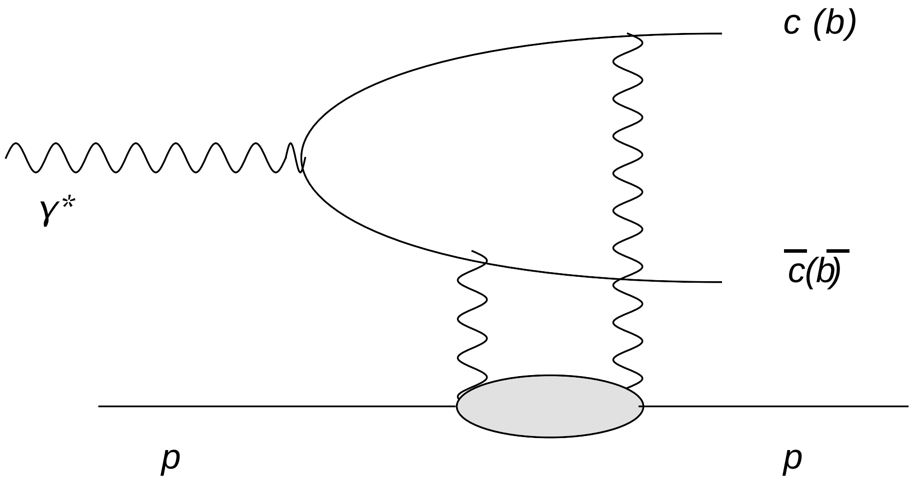

$$\frac{d\sigma_{\gamma^* p \to J/\psi p}}{dt}(W^2, Q^2)\bigg|_{t=0} = \int_{\Delta M^2_{J/\psi}} dM^2 \int_{Z_-}^{Z_+} dz \frac{d\sigma_{\gamma^* p \to (c\bar{c})^{J=1} p}}{dt dM^2 dz}(W^2, Q^2, z, m_c^2, M^2)$$

$$z_\pm = \frac{1}{2} \pm \sqrt{1 - 4\frac{m_c^2}{M^2}}, \qquad \Delta M^2_{J/\psi} \cong 3GeV^2$$

Threshold: $z = \frac{1}{2}; \quad M^2 = 4m_c^2 = M^2_{J/\psi}$

$$\frac{d\sigma_{\gamma^* p \to J/\psi p}(W^2, Q^2)}{dt}\bigg|_{t\cong 0} \propto \frac{(\sigma^{(\infty)}(W^2))^2}{\left(1 + \frac{Q^2 + M^2_{J/\psi}}{\Lambda^2_{sat}(W^2)}\right)^2} \quad \frac{\Delta F^2(m_c^2, \Delta M^2_{J/\psi})}{(Q^2 + M^2_{J/\psi})}$$

$$\cong \begin{cases} \frac{\Lambda^4_{sat}(W^2)(\sigma^{(\infty)}(W^2))^2}{(Q^2+M^2_{J/\psi})^2} \quad \frac{\Delta F^2(m_c^2,\ \Delta M^2_{j/\psi})}{(Q^2+M^2_{J/\psi})}, & \text{for} \quad \frac{Q^2+M^2_{J/\psi}}{\Lambda^2_{sat}(W^2)} \gg 1, \\ (\sigma^{(\infty)}(W^2))^2 \quad \frac{\Delta F^2(m_c^2, \Delta M^2_{J/\psi})}{(Q^2+M^2_{J/\psi})}, & \text{for} \quad \frac{Q^2+M^2_{J/\psi}}{\Lambda^2_{sat}(W^2)} \ll 1. \end{cases}$$

$$\eta_{c\bar{c}}(W^2, Q^2) \equiv \frac{Q^2 + M^2_{J/\psi}}{\Lambda^2_{sat}(W^2)}$$

Photoproduction:

$$\frac{d\sigma_{\gamma p \to J/\psi p}(W^2)}{dt}\bigg|_{t\cong 0} \propto \frac{(\sigma^{(\infty)}(W^2))^2}{\left(1 + \frac{M^2_{J/\psi}}{\Lambda^2_{sat}(W^2)}\right)^2} \frac{\Delta F^2(m_c^2, \Delta M^2_{J/\psi})}{M^2_{J/\psi}}$$

$$\cong \frac{(\sigma^{(\infty)}(W^2))^2 \Delta F^2(m_c^2, \Delta M^2_{J/\psi})}{M^2_{J/\psi}}, \quad \text{for} \quad \eta_{c\bar{c}}(W^2, Q^2 = 0) \ll 1.$$

$\sigma(\gamma^* p \to J/\psi p)$ as a function of Q^2, $\quad W = 90 GeV$.

Kuroda, Schildknecht (2006)

Phys. Lett. B. 638 (2006) 473

$$\sigma(\gamma^* p \to J/\psi p) \sim \frac{1}{(Q^2 + M^2_{J/\psi})^3} \qquad \left(Q^2 + M^2_{J/\psi} \gg \Lambda^2_{sat}(W^2)\right)$$

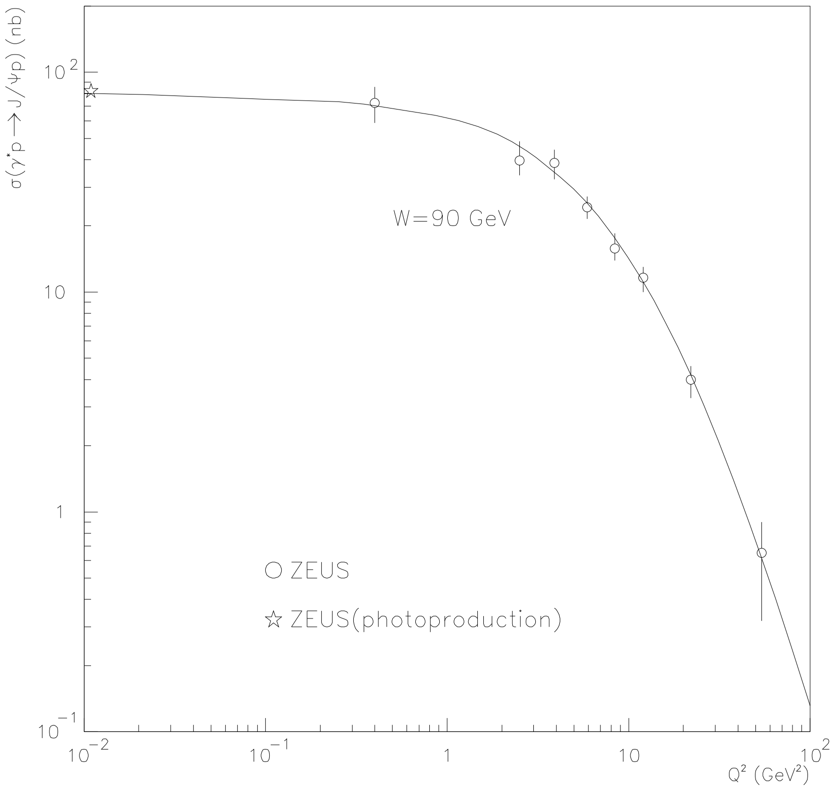

Photoproduction: $\sigma(\gamma p \to J/\psi p) \sim \frac{\Lambda^4_{sat}(W^2)}{\left(1+\frac{\Lambda^2_{sat}(W^2)}{M^2_{J/\psi}}\right)^2}(\ln W^2)^2$

Illustration $\sigma(\gamma p \to J/\psi p) \sim \Lambda^4_{sat}(W^2)$

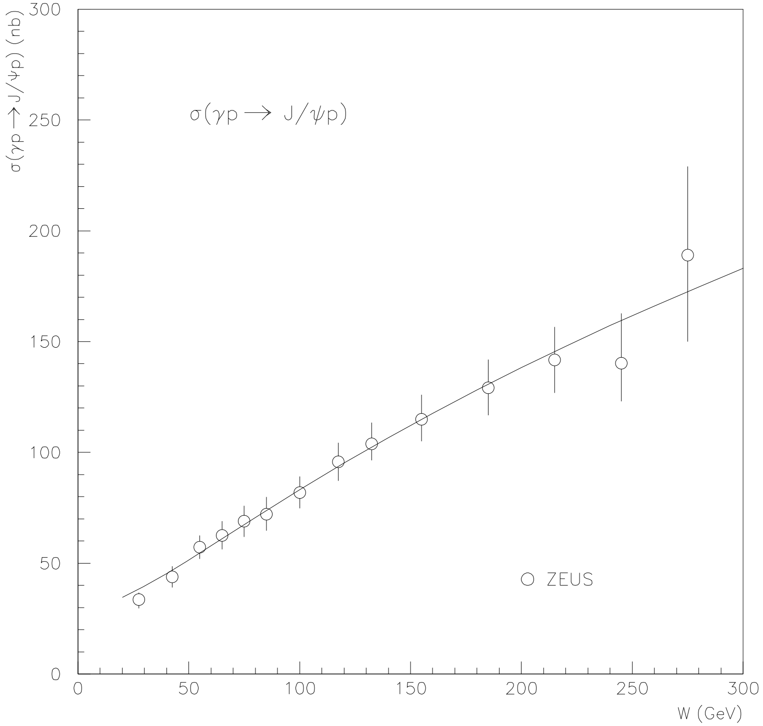

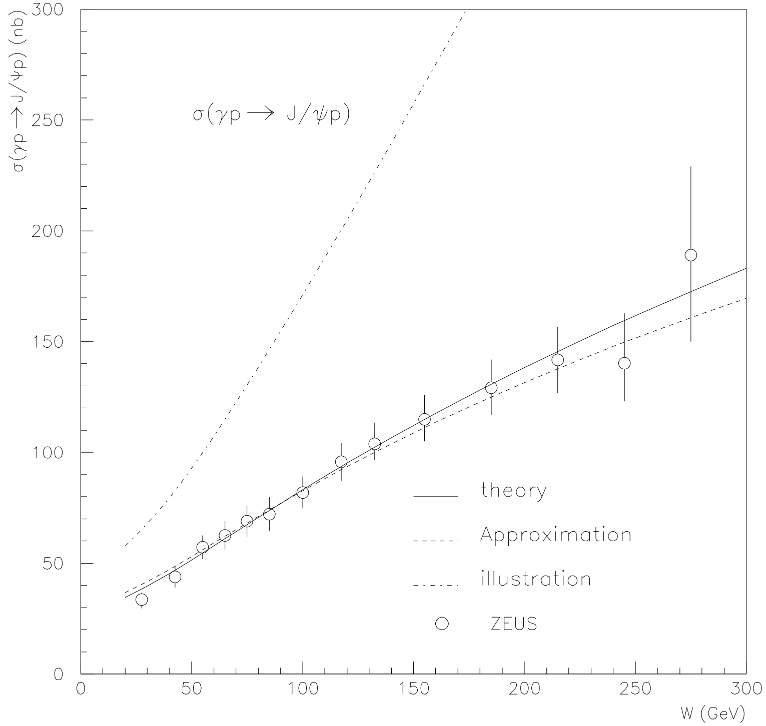

J/ψ Photoproduction at LHCb

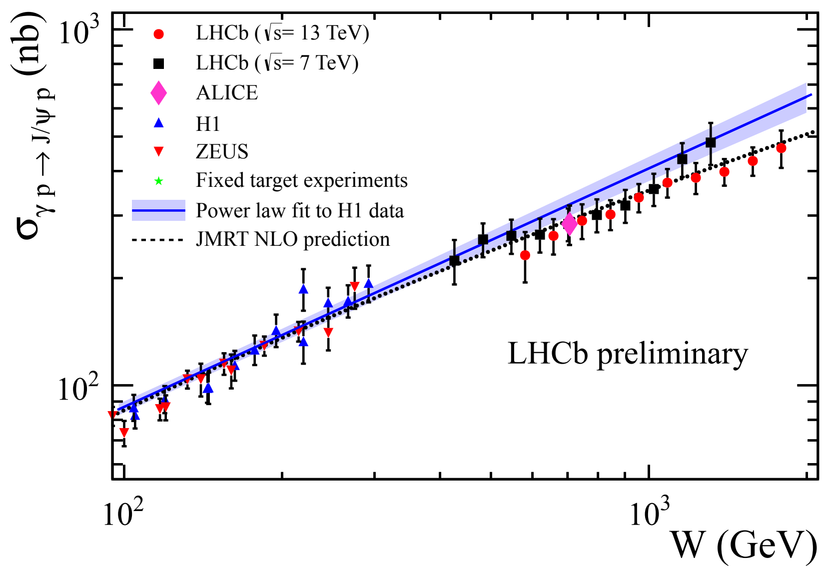

D. Schildknecht, Phys. Lett. B, 2016

$$\sigma_{\gamma p\to J/\psi p}(W^2) = \frac{\left(1+\frac{M^2_{J/\psi}}{\Lambda^2_{sat}(W_1^2)}\right)^2}{\left(1+\frac{M^2_{J/\psi}}{\Lambda^2_{sat}(W^2)}\right)^2}\frac{\left(\sigma^{(\infty)}(W^2)\right)^2}{\left(\sigma^{(\infty)}(W_1^2)\right)^2}\sigma_{\gamma p\to J/\psi p}(W_1^2=(100GeV)^2),$$

$$\equiv F_A(\Lambda^2_{sat}(W^2))F_B(W^2)\sigma_{\gamma p\to J/\psi p}(W_1^2=(100GeV)^2),$$

$W[GeV]$	$\Lambda^2_{sat}(W^2)[GeV^2]$	$\frac{M^2_{J/\psi}}{\Lambda^2_{sat}(W^2)}$	$F_A(\Lambda^2_{sat}(W^2))$	$F_B(W^2)$	$\sigma_{\gamma p\to J/\psi p}(W)[nb]$
100	4.32	2.22	1	1	80
300	7.92	1.21	2.12	1.02	173
1000	15.4	0.624	3.93	1.11	349
2000	22.6	0.425	5.11	1.16	474

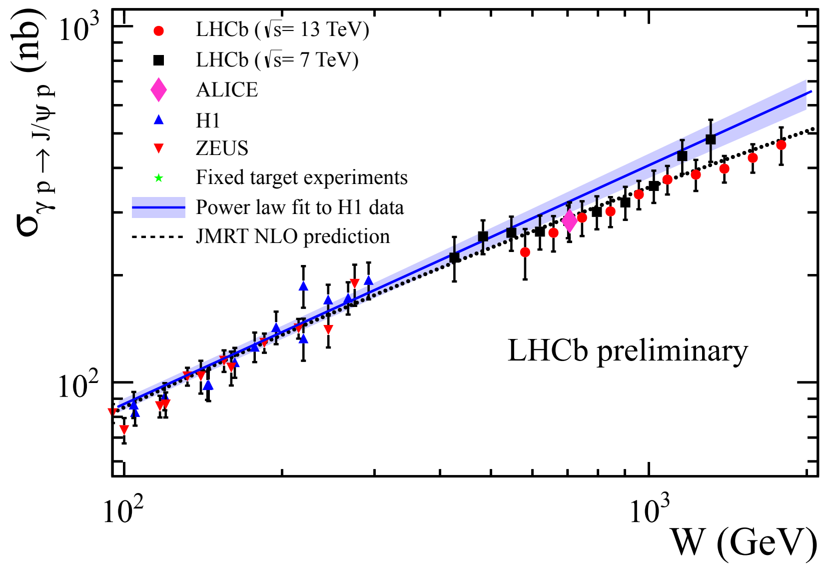

$W\,[GeV]$	$\Lambda^2_{sat}(W^2)[GeV^2]$	$\frac{M^2_{J/\psi}}{\Lambda^2_{sat}(W^2)}$	$F_A(\Lambda^2_{sat}(W^2))$	$F_B(W^2)$	$\sigma_{\gamma p\to J/\psi p}(W)[nb]$
100	4.32	2.22	1	1	80
300	7.92	1.21	2.12	1.02	173
1000	15.4	0.624	3.93	1.11	349
2000	22.6	0.425	5.11	1.16	474

LHCb experimental results correspond to

$$\mathbf{2.2} \gtrsim \eta_{c\bar{c}}(W^2, Q^2 = 0) \gtrsim \mathbf{0.43},$$

transition from color transparency to saturation.

6. The Neutrino-Nucleon Cross Section in the CDP

$$\sigma_{\nu N}(E) = \frac{G_F^2 M_W^4}{8\pi^3\alpha}\frac{n_f}{\sum_q Q_q^2}\int_{Q^2_{Min}}^{s-M_p^2} dQ^2 \frac{Q^2}{(Q^2+M_W^2)^2} \times \int_{M_p^2}^{s-Q^2}\frac{dW^2}{W^2}\frac{1}{2}(1+(1-y)^2)\sigma_{\gamma^* p}(\eta(W^2,Q^2)).$$

Kuroda, Schildknecht, arXiv:1305.0440v3, Phys. Rev. D88 (2013) 053007

$$r(E) = \frac{\sigma_{\nu N}(E)_{\eta(W^2,Q^2)<1}}{\sigma_{\nu N}(E)}.$$

Contribution from saturation region

$$r(E) < \bar{r}(E),$$

$$\bar{r}(E) = \frac{2\int_{Q^2_{Min}}^{Q^2_{Max}(s)} dQ^2 \frac{Q^2}{(Q^2+M_W^2)^2}\int_{W^2(Q^2)_{Min}}^{s-Q^2}\frac{dW^2}{W^2}\ln\frac{1}{\eta(W^2,Q^2)}}{\int_{Q^2_{Min}}^{s-M_p^2} dQ^2 \frac{Q^2}{(Q^2+M_W^2)^2}\int_{M_p^2}^{s-Q^2}\frac{dW^2}{W^2}\frac{1}{2\eta(W^2,Q^2)}}.$$

$$r(E) < \bar{r}(E) = \frac{1}{2}\frac{\Lambda^2_{sat}(s)}{M_W^2} = \begin{cases} 1.74\times 10^{-3} & \text{for } E = 10^6\,\text{GeV} \\ 2.51\times 10^{-2} & \text{for } E = 10^{10}\,\text{GeV} \\ 3.63\times 10^{-1} & \text{for } E = 10^{14}\,\text{GeV} \end{cases}.$$

Note: Ice Cube Experiment, $E \lesssim 10^6 GeV$

The (charged-current) neutrino-nucleon cross section, $\sigma_{\nu N}(E)$, (based on $\sigma_{\gamma^* p}(\eta(W^2, Q^2))$ from CDP) as a function of the neutrino energy $E_\nu(GeV)$.

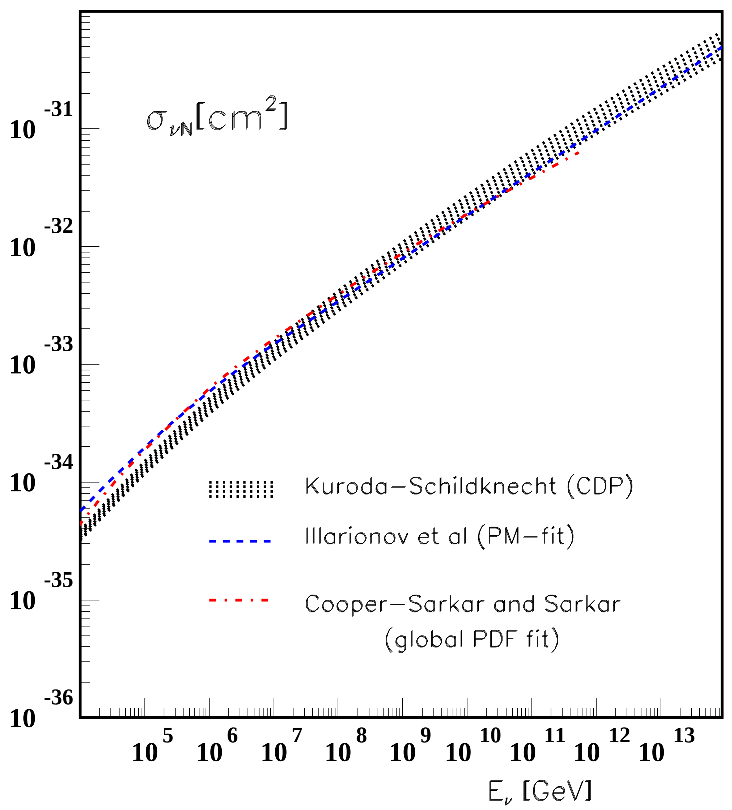

7. Conclusions

Deep Inelastic Scattering (DIS)

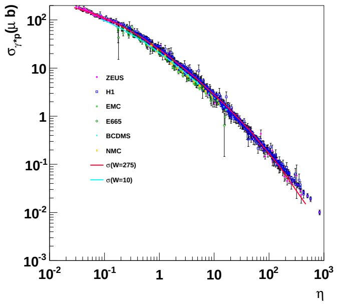

- The empirically observed low-x $\left(x_{bj} \cong \frac{Q^2}{W^2} \leq 0.1\right)$ scaling behavior,

$$\sigma_{\gamma^* p}(W^2, Q^2) = \sigma_{\gamma^* p}\left(\eta(W^2, Q^2)\right),$$

where $\eta(W^2, Q^2) = \frac{Q^2 + m_0^2}{\Lambda^2_{\text{sat}}(W^2)}$,

$$\Lambda^2_{\text{sat}}(W^2) = C_1 \left(\frac{W^2}{1\text{GeV}^2}\right)^{C_2},$$

is a consequence of the color-gauge-invariant $q\bar{q}$-dipole interaction with the color field in the nucleon.

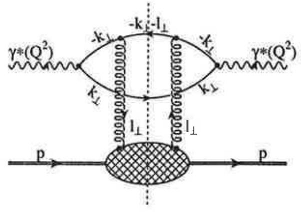

(a)

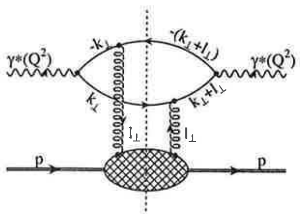

(b)

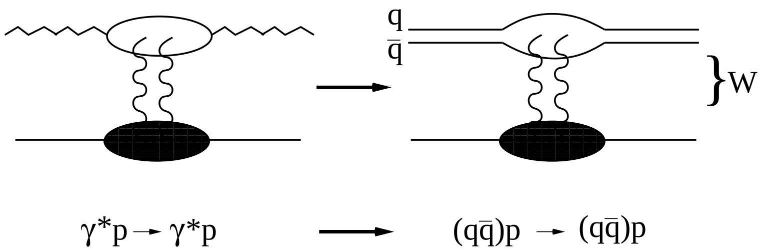

- For $\eta(W^2, Q^2) \gg 1$, color transparency, $\sigma_{(q\bar{q})p} \sim \vec{r}_\perp^{\,2}$, implies $\sigma_{\gamma^* p} \sim \frac{1}{\eta}$.

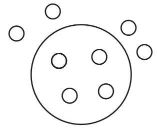

- For $\eta(W^2, Q^2) \ll 1$, saturation, $\sigma_{(q\bar{q})p} \sim \sigma^{(\infty)}(W^2)$, implies $\sigma_{\gamma^* p} \sim \sigma^{(\infty)}(W^2) \ln \frac{1}{\eta}$, i. e. hadronlike $\ln^2 W^2$ dependence at any Q^2 fixed.

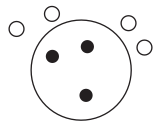

- $R(W^2, Q^2) = \frac{\sigma_{\gamma_L^* p}(\eta(W^2,Q^2))}{\sigma_{\gamma_T^* p}(\eta(W^2,Q^2))} = \frac{1}{2\rho}$ for $\eta \gg 1$.

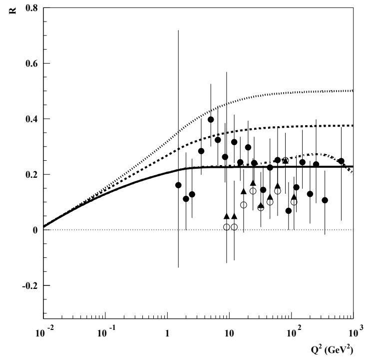

- Detailed model essentially based on a parameterization of

$$\Lambda_{\text{sat}}^2(W^2) = C_1 \left(\frac{W^2}{1\text{GeV}^2} \right)^{C_2}$$

shows agreement with all DIS data at low x, including $Q^2 = 0$ photoproduction.

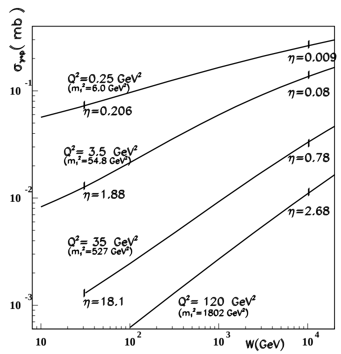

- $q\bar{q}$ mass range for $(1-\epsilon)$ fraction of cross section $m_0^2 \leq M_{q\bar{q}}^2 \leq \frac{3}{2\epsilon}(Q^2 + m_0^2)$.

J/ψ and Y

- Applying quark-hadron duality to $c\bar{c}$ and $b\bar{b}$ photo- and electroproduction yields parameter-free predictions for J/ψ and Y production.
- The presently observed strong rise with energy saturates into a $(log W^2)^2$ dependence at asymptotic (ultrahigh) energies.

Neutrino-Nucleon Cross Section

- Predictions for the charged-current neutrino-nucleon cross section based on the CDP are consistent with results obtained from pQCD fits ($E \leq 10^{12}$ GeV).